

Effects of Lubrication on the Friction in Nanometric Machining Processes: A Molecular Dynamics Approach

Martin P. Lautenschlaeger^{1,a}, Simon Stephan¹, Herbert M. Urbassek², Benjamin Kirsch³, Jan C. Aurich³, Martin T. Horsch¹, and Hans Hasse¹

¹Laboratory of Engineering Thermodynamics (LTD), University of Kaiserslautern, 67663 Kaiserslautern, Germany

²Physics Department and Research Center OPTIMAS, University of Kaiserslautern, 67663 Kaiserslautern, Germany

³Institute for Manufacturing Engineering and Production Management (FBK), University of Kaiserslautern, 67663 Kaiserslautern, Germany

^aMartin.Lautenschlaeger@mv.uni-kl.de

Keywords: Cutting, Grinding, Friction, Indentation, Lubricant, Dissipation, Molecular Dynamics Simulation, Solid-Fluid Interface

Abstract. Physical phenomena in a nanometric machining process were studied by molecular dynamics simulations. A cylindrical tool was indented and then moved laterally on an initially flat workpiece. The focus of the study is on the effect of lubrication on the nanoscale. Therefore, the indentation and the scratching were studied both in vacuum and submersed in a lubricant. All materials were modeled by Lennard-Jones truncated and shifted potential sites. It is observed, that in the lubricated case, a substantial part of the cutting edge of the tool is in dry contact with the workpiece. Nevertheless, compared to the dry scenario, the lubrication lowers the coefficient of friction. However, the work which is needed for the indentation and the scratching is not reduced. The processed surface is found to be smoother in the lubricated case. As expected, the lubrication has an important influence on the temperature field observed in the simulation.

Introduction

Ultra precision machining processes play an important role in creating miniaturized surface structures. In advanced optical and photonic products the tolerances which must be met by these processes approach the atomic length scale. The substrates are processed by removing atoms almost layer by layer to get a precision in the order of nanometers [1].

The physical phenomena during such nanometric machining processes are not yet fully understood. They may differ significantly from those on the macroscale and are hard to study experimentally. Molecular dynamics simulations provide an attractive and appropriate way to study nanometric machining processes and thus, to gain a better understanding. The results of molecular dynamics simulations are achieved by solving Newton's equations of motion for a given scenario and are solely based on the force field which describes the interactions on the atomistic level. They provide information in atomistic resolution.

Molecular dynamics simulations have been used before for studies of tool-workpiece interactions, e.g. [2–7]. The focus in most of these studies was on chip formation, the topology of the resulting surface, and the creation of dislocations in the workpiece. However, in most of the available studies only solid-solid interactions are considered, i.e. tool and workpiece interact in vacuum, there is no lubrication. There are only a few molecular dynamics studies which consider the effect of lubricants on nanometric machining [1, 8–12]. Each of them focusses on the description of a certain substrate-fluid pair and usually no special attention is given to the influence of the substrate-fluid interaction, even though that interaction plays a predominant role in such processes [13, 14]. Therefore, in the present work, a molecular dynamics study of the effect of lubrication in a nanometric machining

process was carried out using a model system which allows systematic studies of the influence of the substrate-fluid interaction. Since, the two primary tasks of lubrication are the reduction of friction and the cooling, both were investigated, with a focus on the mechanical effects.

As the results apply not only to machining, the following more general designations are used here: lubricant = fluid (F), tool = indenter (I), workpiece = substrate (S).

Modelling and Simulation Setup

Molecular Model. The fluid, the substrate and the indenter are represented by suitably parametrized Lennard-Jones truncated and shifted (LJTS) potentials $u^{\text{LJTS}}(r_{ij})$. LJTS models of fluids have been studied in great detail and are known to reproduce thermo-physical properties of simple nonpolar fluids accurately [15, 16]. LJTS models were also used before for studying solid-liquid contacts. E.g. in [13], the wetting of solids was systematically investigated using LJTS models for representing the liquid and the gas, as well as the solid. The simple LJTS potential is, however, not suited for appropriately describing details of the solid's behavior like dislocations.

The LJTS potential is:

$$u^{\text{LJTS}}(r_{ij}) = \begin{cases} u^{\text{LJ}}(r_{ij}) - u^{\text{LJ}}(r_c), & r_{ij} < r_c \\ 0, & r_{ij} \geq r_c \end{cases}, \quad (1)$$

where

$$u^{\text{LJ}}(r_{ij}) = 4\epsilon[(\sigma/r_{ij})^{12} - (\sigma/r_{ij})^6], \quad (2)$$

ϵ is the energy parameter, describing dispersive attraction and σ is the size parameter describing the repulsion. r_{ij} is the distance between two LJTS sites i and j and r_c is the cut-off radius, which is the maximal distance for which the attraction is considered.

The parameterization which is presented below results from preliminary test runs with different parameterizations. In follow-up work systematic parameter variations will be carried out.

In the present study, the size parameters of all LJTS sites σ are the same, and all sites have the same mass M . The size parameter σ is also used to normalize all distances. The energy is normalized using the LJTS energy parameter of the fluid $\epsilon = \epsilon_F$. The cohesive energy of the workpiece is set to $\epsilon_S = 52 \epsilon$ mimicking a ratio that is similar to the ratio of argon or methane and a common metal like iron or vanadium [17]. The LJTS sites of the fluid are unconstrained, and a cut-off radius of 2.5σ is chosen. The same holds for the substrate, except for the fixation layers at the border of the simulation box (see below). In contrast, the movement of the LJTS sites of the indenter regarding their velocity and direction is fully prescribed, i.e. the indenter is rigid. Following the Lorentz rule, the size parameters are σ also for the unlike interactions. The energy parameter of the substrate-fluid interaction is $\epsilon_{\text{SF}} = 0.5 \epsilon$, which corresponds to a contact angle of about 90° according to *Becker et al.* [13]. The same value is chosen for the indenter-fluid interaction: $\epsilon_{\text{IF}} = 0.5 \epsilon$. For the substrate-indenter interaction the value is $\epsilon_{\text{SI}} = 2.5 \epsilon$. The cut-off radius is again 2.5σ for the unlike interactions, except of the substrate-indenter interaction, that was kept purely repulsive by setting the cut-off $r_{\text{c,SI}} = 1.0 \sigma$, cf. [18].

All simulations were carried out using LAMMPS [19]. All observables are given in reduced units, cf. Table 1. The time step that was used is $\Delta\tau = 0.006$.

Simulation Scenario. Fig. 1 depicts the simulation scenario. It consists of the rigid indenter (I) that models the cutting edge of a tool, a solid substrate (S), and eventually a fluid lubricant (F). The simulation box dimensions are $l_x = 309$, $l_y = 71$, and $l_z = 295$. The indenter is a cylinder with the radius $R = 9$ and the length $L = 71$. $x = 0$ indicates the initial position of the indenter which is kept constant during the indentation. $z = 0$ indicates its position when the distance between the center of the indenter and the initial, flat substrate surface is equivalent to the indenter's radius R . I.e. the origin of the z -axis

Table 1: Definitions of the observables in reduced units. The asterisk indicates the corresponding observable carrying a dimension. k_B is the Boltzmann's constant.

Length	$x = x^*/\sigma$
Time	$\tau = \tau^*/(\sigma\sqrt{M/\varepsilon})$
Mass	$m = m^*/M$
Temperature	$T = T^*/(\varepsilon/k_B)$
Pressure	$p = p^*/(\varepsilon/\sigma^3)$
Velocity	$v = v^*/(\sqrt{\varepsilon/M})$
Force	$F = F^*/(\varepsilon/\sigma)$
Work	$W = W^*/\varepsilon$

corresponds to the position of the indenter's center, when the indenter firstly touches the substrate. In the initial situation, the substrate is a fcc lattice with the particle density $\rho_S = 1.07$. The numbers of LJTS sites are about $1.71 \cdot 10^6$ for the fluid, $1.67 \cdot 10^4$ for the indenter, and $3.16 \cdot 10^6$ for the substrate. The substrate is fixed in the box by fixing the two layers of substrate sites next to the box margins. For the fluid, periodic boundary conditions are used in x - and y -direction, while in z -direction a soft repulsive boundary condition is used. The initial temperature and pressure of the equilibrated system are $T = 0.8$ and $p = 0.005$, respectively. The temperature is also imposed to the lowest three layers of LJTS sites of the substrate next to the fixed layers by velocity scaling. Throughout the entire simulation, there is no evaporation, i.e. the lubricant is always liquid.

In the initial situation, the center of the indenter is located at $x = 0$ and $z = 5.5$. The indenter then conducts two sequential movements: first, it moves in negative z -direction, and penetrates the substrate until the center of the indenter has reached $z = -4.5$. Then, at constant z , the indenter moves laterally up to $x = 35$. The indenter speed is $v = 0.12$ for both movements.

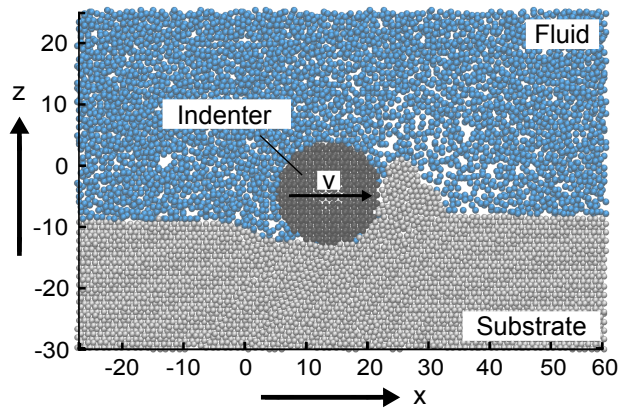


Fig. 1: Schematic view of the simulation scenario with fluid, indenter, and substrate, representing a nanometric machining process in the close vicinity of the cutting edge. After the indentation in negative z -direction, the indenter is moved at constant velocity $v = 0.12$ in x -direction forming a chip. The scheme shows only a small part of the whole simulation box with focus on the contact region.

Simulational Results

A snapshot of a simulation with lubricant is shown in Fig. 1. It was taken in the middle of the lateral movement of the indenter. There is a pile-up of material in front of the indenter, i.e. a chip is formed. Also the stacking faults in the substrate are visible. Furthermore, as only a thin slice in y -direction

is shown, the lowering of the density of the fluid in the zone near the chip, where the temperature is high, can be seen. One of the most striking features of the simulation is, that there are hardly any fluid particles in the contact zone between the indenter and the substrate. That phenomenon has already been observed by *Rentsch et al.* [8] as well as by *Childs* [20], who reports that for scratching velocities of the order of m/s the stresses in the contact region are too high for the fluid to penetrate into it. To illustrate the results, which are presented in dimensionless variables here, Table 2 shows the results of the transformation of some of the key properties to variables carrying dimensions. For that purpose, the LJTS parameters of argon as reported by *Vrabec et al.* [21] were used.

Table 2: Overview of characteristic system properties in quantities carrying dimensions. The reduced units listed in the text are converted using the following model for argon [21]: $\sigma_F = 0.33916$ nm, $\epsilon_F = 137.9$ K, and $M_F = 6.64 \cdot 10^{-26}$ kg.

Observable	Real unit
System size	105·24·100 nm ³
Time step	1.2 fs
Initial pressure	2.4 bar
Initial temperature	110.3 K
Substrate density	1.82 g/cm ³
Indenter radius	3.0 nm
Indentation depth	1.5 nm
Scratching velocity	20.0 m/s
Scratching distance	11.9 nm

Indenter Forces. The total forces acting on the indenter during the two phases of the machining process are shown in Fig. 2 for both the dry and the lubricated case. The top panel of Fig. 2 shows the force in z -direction for the indentation phase, the middle panel shows the force in z -direction for the scratching phase, and the bottom panel shows the negative force in x -direction for the scratching phase.

During the indentation phase, after the first contact is established, the force in z -direction acting on the indenter rises almost linearly yet with some fluctuations, cf. Fig. 2 top panel. The shift between the curves for the dry and the lubricated case is a direct result of the presence of fluid particles between the indenter and the substrate in the latter case. They also give rise to a dampening effect which reduces the fluctuations compared to the dry case. The fluctuations show a pattern that reflects the influence of the substrate's lattice layer structure. In the early phase of the contact in the lubricated case, the influence of the adsorbed fluid layer on the surface is discernible. This is in line with the results of *Vo et al.* [22] who report an important increase of the viscosity of fluids near solid walls.

The middle panel of Fig. 2 shows the force in z -direction acting on the indenter F_z during scratching. Two phases can be discerned: first F_z decreases. This results from settling processes in the substrate which lead to a reduction of the stresses. This also explains why there is no significant difference between the results for the lubricated and the dry case in most of that phase. In the second phase, the force F_z has reached a level and basically only fluctuates as the indenter moves forwards. The characteristics of these fluctuations differ between the dry and the lubricated case, which could indicate a dampening by the fluid.

The force in negative x -direction acting on the indenter in the scratching phase is shown in the bottom panel of Fig. 2. There is an initial rise of that force which is faster for the dry case than for the lubricated case, since, for the latter, first fluid atoms are squeezed out of the contact region. Then the force F_x fluctuates in a broad band as the indenter moves forward, with no significant differences between the lubricated and the dry case. There is an important influence of lattice deformations in the substrate which are not influenced by the lubrication.

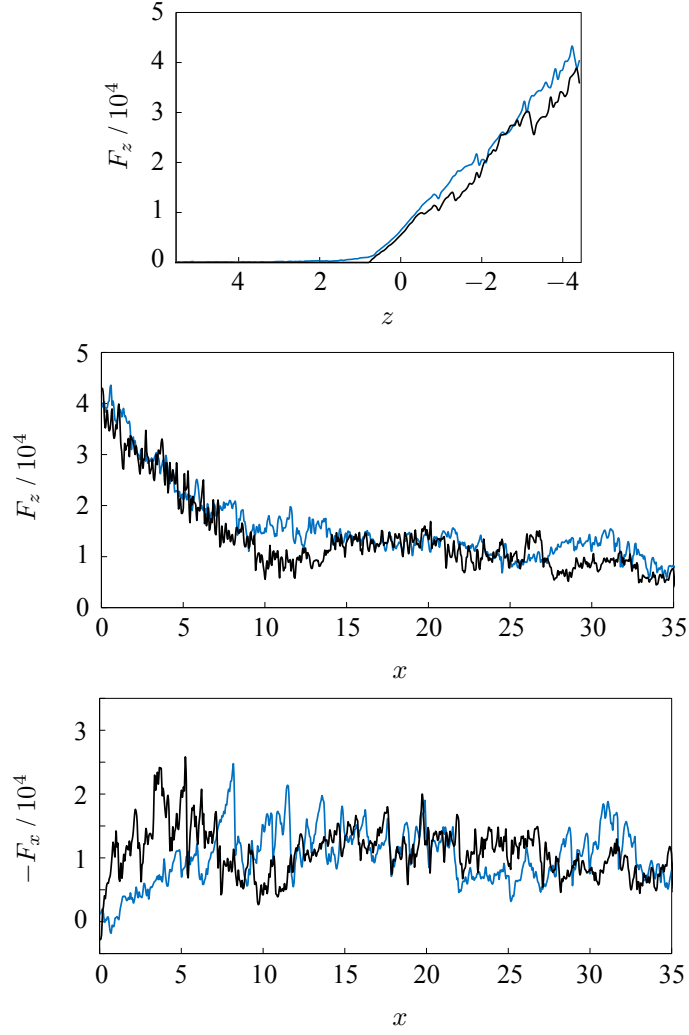


Fig. 2: Forces acting on the indenter during the studied nanometric machining process for the lubricated case (blue lines) and the dry case (black lines). Top: Force in z -direction F_z as a function of the indentation length z . Middle: Force in the z -direction F_z as a function of the scratching length x . Bottom: Force in the negative x -direction $-F_x$ as a function of the scratching length x .

Fig. 2 shows that for scratching lengths above about 10, a steady state regarding averaged values is reached. Therefore, for that phase, averaged values of all mechanical observables were calculated for both the dry and the lubricated case. This corresponds to an averaging over 350,000 time steps. The result is shown in Table 3.

The absolute values of the average forces on the indenter, both in z - and $-x$ -direction are higher for the lubricated scenario than for the dry one. However, the deviations are still within the standard deviations of both data sets, which are in a range between 25% and 35% here. From the average values, the coefficient of friction $\text{COF} = |F_x/F_z|$ can be calculated. For results see Table 3. The COF is found to be slightly lower for the lubricated case, mainly due to the higher magnitude of F_z . However, in interpreting that difference, the large scattering of the primary data must be considered. *Chen et al.* [10] also observed a lowering of the COF by lubrication in atomistic simulations of nanometric machining for the same reason. The scratching work is calculated from an integration of the force F_x over the path x for the steady state process, i.e. between $x_1 = 10$ and $x_2 = 35$. In accordance with the above, it is found to be slightly higher for the lubricated case than for the dry one, cf. Table 3. However, the difference between both cases is not significant.

Surface Structure. To study the creation of a new surface by the machining process, the surface of the substrate and that of the indenter is tracked. For the determination of the substrate surface geometric

Table 3: Comparison of the results of the dry and the lubricated scratching simulations by averaged numbers for the steady state phase of the scratching process.

	dry	lubricated
Force in z -direction	$1.08 \cdot 10^4$	$1.32 \cdot 10^4$
Force in $-x$ -direction	$1.05 \cdot 10^4$	$1.12 \cdot 10^4$
Coefficient of friction	0.97	0.85
Scratching work	$31.2 \cdot 10^4$	$33.3 \cdot 10^4$
Confinement volume	616.5	650.8
Relative surface enlargement	14 %	7 %

criteria adapted to the scenario are used, which here were found to be more efficient than general criteria like the alpha shape method [23].

The creation of a new surface is a result of the interaction of the indenter with the substrate. The confined volume between these two bodies is a measure for characterizing that interaction. The definition of that volume is illustrated in Fig. 3. In the stationary period of the scratching, the confinement volume is only marginally higher in the lubricated case compared to the dry one, cf. Table 3. This illustrates that there is hardly any lubricant in the direct contact zone.

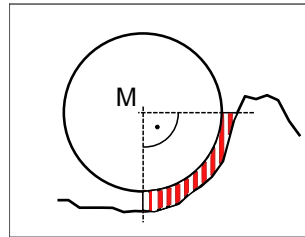


Fig. 3: Illustration of the definition of the confinement volume between the indenter and the substrate, cf. the red shaded area. Here, M designates the rotation axis of the indenter.

Furthermore, the structure of the created surface is analyzed. As a simple measure, the ratio of the actual substrate surface area after the machining and the initial surface area before the machining is calculated. For that purpose only the part of the surface which is affected by the machining is considered, without, however, considering the chip. This is illustrated in Fig. 4 which also gives results for the surface structure for the dry and the lubricated case. The increase of the surface area is higher for the dry than for the lubricated case, cf. Table 3. This results mainly from the increased roughness of the surface in the dry case, cf. Fig. 4.



Fig. 4: Surface structure for the dry case (left) and the lubricated case (right). The red line indicates the part of the surface which was considered for the calculation of the surface area after the machining and hence, for the relative surface enlargement where it was compared to the flat initial surface area.

Temperature Distribution. Snapshots of the temperature field in the system taken during the steady state scratching operation (for $x = 17$) in the dry and the lubricated case are presented in Fig. 5. In the

dry case, the chip heats up very strongly. Cooling takes place only by heat conduction in the solid. In the lubricated case, the fluid contributes significantly to the cooling. The fluid layers which are adsorbed at the solid surfaces play an important role in the thermal processes in nanoscale machining.

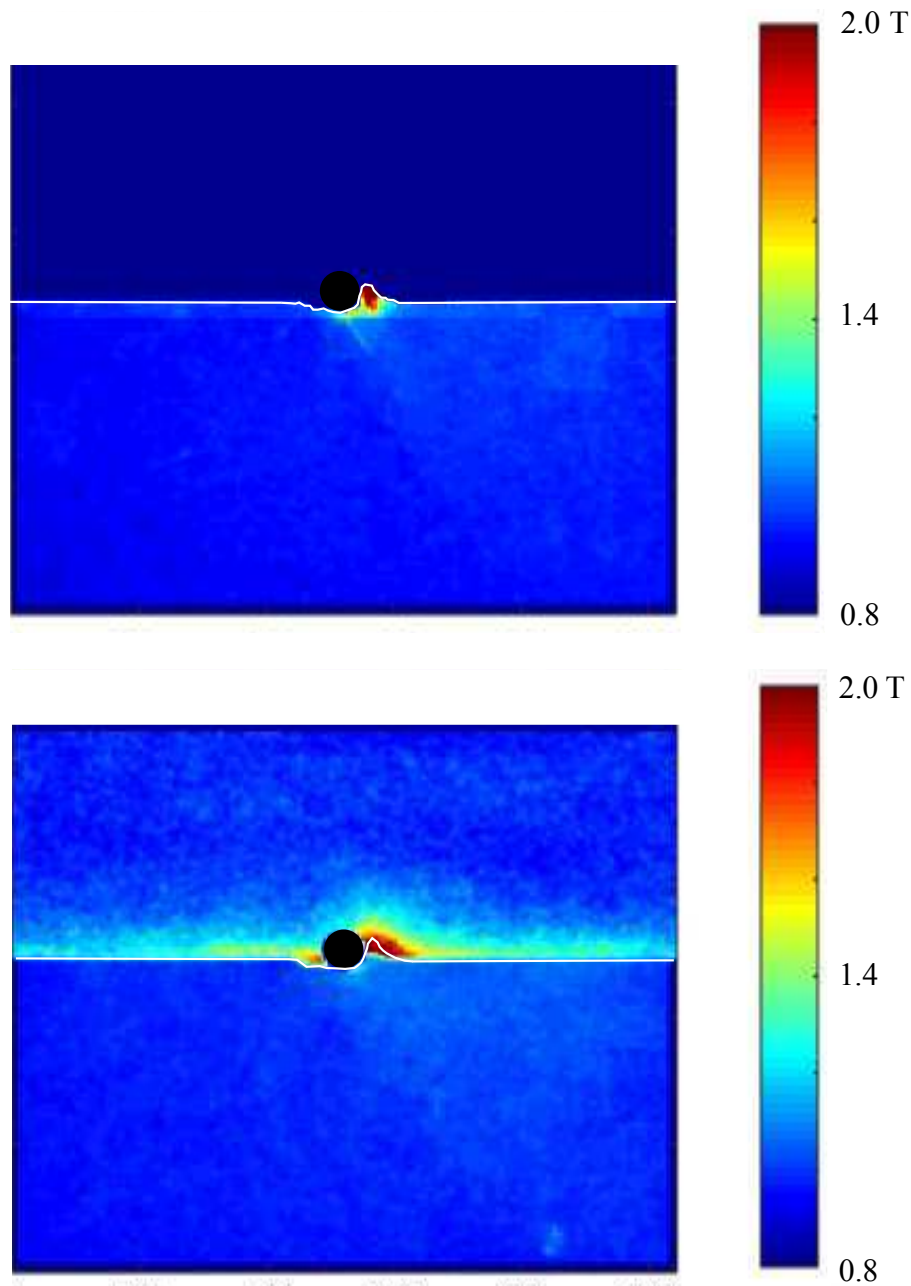


Fig. 5: Temperature field in the simulation box in the dry case (top) and the lubricated case (bottom). The white lines indicate the substrate surface. The indenter is depicted as a black circle. The vacuum and the fixed and thermostated substrate layers at the boundaries are depicted in dark blue.

The findings from the present study differ significantly from those of *Rentsch et al.* [8], who also studied lubricated nanometric machining, but used a scenario in which the fluid was held at constant temperature in the simulation, whereas in our simulations only the bottom and lateral faces of the substrate were thermostated. *Chen et al.* [9, 10] also report high temperatures in chips formed in nanometric machining.

Conclusion

In the present work, molecular dynamics simulations are used to study the influence of lubrication on a nanometric machining process in which an indenter first penetrates a workpiece vertically and then scratches the surface laterally. Two scenarios are compared: a dry one and one in which an indenter and a substrate are immersed in a lubricant. All objects are modeled by suitably parameterized LJTS potentials. The results show that for the given substrate-fluid and indenter-fluid interaction there is hardly any lubricant in the contact zone between the indenter and the substrate in which the new surface is formed. As expected, lubrication has an important influence in the thermal processes. A positive effect of lubrication on the smoothness of the created surface is observed. The results for the mechanical properties obtained for the dry and the lubricated case differ only slightly. A minor decrease of the coefficient of friction in the lubricated case, which was observed, seems to be related rather to an increase in the vertical force than to a decrease in the lateral force during scratching. The present work is a case study in which a way to carry out molecular dynamics simulation studies of nanometric machining is developed and tested. That way is shown to be feasible and to yield interesting results. However, in the present work, only a single parameter combination was studied. Systematic studies following the way which is described here are feasible and attractive and will be the topic of future work of our group.

Acknowledgement

The authors gratefully acknowledge financial support by the DFG within IRTG 2057 "Physical Modelling for Virtual Manufacturing Systems and Processes". The simulations were carried out at High Performance Computing Center Stuttgart (HLRS) and Regional University Computing Center Kaiserslautern (RHRK). The present research was conducted under the auspices of the Boltzmann-Zuse Society of Computational Molecular Engineering (BZS).

References

- [1] Goel, S. ; Luo, X. ; Agrawal, A. ; Reuben, R.: Diamond Machining of Silicon: A Review of Advances in Molecular Dynamics Simulation. In: *Int. J. Mach. Tool and Manuf.* 88 (2015), S. 131–164
- [2] Gao, Y. ; Urbassek, H.: Evolution of plasticity in nanometric cutting of Fe single crystals. In: *Applied Surface Science* 317 (2014), S. 6–10
- [3] Aristizibal, H. ; Parra, P. ; López, P. ; Restrepo-Parra, E.: Atomistic-Scale Simulations of Material Behaviors and Tribology Properties for BCC Metal Films. In: *Chin. Phys. B* 25 (2016), S. 010204
- [4] Cho, M. ; Kim, S. ; Lim, D. ; Jang, H.: Atomistic Scale Stick-Slip Caused by Dislocation Nucleation and Propagation During Scratching of a Cu Substrate With a Nanoindenter: A Molecular Dynamics Simulation. In: *Wear* 259 (2005), S. 1392–1399
- [5] Gao, Y. ; Lu, C. ; Huynh, N. ; Michal, G. ; Zhu, H. ; Tieu, A.: Molecular Dynamics Simulation of Effect of Indenter Shape on Nanoscratch of Ni. In: *Wear* 267 (2009), S. 1998–2002
- [6] Wu, C. ; Fang, T. ; Lin, J.: Atomic-scale Simulations of Material Behaviors and Tribology Properties for FCC and BCC Metal Films. In: *Material Letters* 80 (2012), S. 59–62
- [7] Zhang, L. ; Zhao, H. ; Yang, Y. ; Huang, H. ; Ma, Z. ; Shao, M.: Evaluation of Repeated Single-point Diamond Turning on the Deformation Behavior of Monocrystalline Silicon via Molecular Dynamic Simulations. In: *Applied Physics A* 116 (2014), S. 141–150

- [8] Rentsch, R. ; Inasaki, I.: Effects of Fluids on the Surface Generation in Material Removal Processes - Molecular Dynamics Simulation -. In: *Annals of the CIRP* 55 (2006), S. 601–604
- [9] Chen, R. ; Liang, M. ; Luo, J. ; Lei, H. ; Guo, D. ; Hu, X.: Comparison of Surface Damage Under the Dry and Wet Impact: Molecular Dynamics Simulation. In: *Applied Surface Science* 258 (2011), S. 1756–1761
- [10] Chen, Y. ; Han, H. ; Fang, F. ; Hu, X.: MD Simulation of Nanometric Cutting of Copper With and Without Water Lubrication. In: *Science China* 57 (2014), S. 1154–1159
- [11] Ren, J. ; Zhao, J. ; Dong, Z. ; Liu, P.: Molecular Dynamics Study on the Mechanism of AFM-based Nanoscratching Process With Water-layer Lubrication. In: *Applied Surface Science* 346 (2015), S. 84–98
- [12] Tang, C. ; Zhang, L.: A Molecular Dynamics Analysis of the Mechanical Effect of Water on the Deformation of Silicon Monocrystals Subjected to Nano-Indentation. In: *Nanotechnology* 16 (2005), S. 15–20
- [13] Becker, S. ; Urbassek, H. ; Horsch, M. ; Hasse, H.: Contact Angle of Sessile Drops in Lennard-Jones Systems. In: *Langmuir* 30 (2014), S. 13606–13614
- [14] Yan, P. ; Rong, Y. ; Wang, G.: The Effect of Cutting Fluids Applied in Metal Cutting Process. In: *J. Engineering Manufacture* 230 (2016), S. 19–37
- [15] Allen, M. ; Tildesley, D.: *Computer Simulations of Liquids*. Oxford, 2009
- [16] Karniadakis, G. ; Beskok, A. ; Aluru, N.: *Microflows and Nanoflows*. Bd. Second Edition. New York : Springer-Verlag, 2005
- [17] Zhen, S. ; Davies, G.: Lennard-Jones n-m Potential Energy Parameters. In: *Phys. Stat. Sol.* 78 (1983), S. 595
- [18] Kelchner, C. ; Plimpton, S. ; Hamilton, J.: Dislocation Nucleation and Defect Structure During Surface Indentation. In: *Phys. Rev. B* 58 (1998), S. 11085–11088
- [19] Plimpton, S.: Fast Parallel Algorithms for Short-Range Molecular Dynamics. In: *J. Comp. Phys.* 117 (1995), S. 1–19. – 17.11.2016
- [20] Childs, T.: Friction Modelling in Metal Cutting. In: *Wear* 260 (2006), S. 310–318
- [21] Vrabc, J. ; Kedia, G. ; Fuchs, G. ; Hasse, H.: Comprehensive Study of the Vapour–liquid Coexistence of the Truncated and Shifted Lennard–Jones Fluid Including Planar and Spherical Interface Properties. In: *Molecular Physics* 104 (2006), S. 1509–1527
- [22] Vo, T. ; Park, B. ; Park, C. ; Kim, B.: Nano-Scale Liquid Film Sheared Between Strong Wetting Surfaces: Effects of Interface Region on the Flow. In: *J. Mech. Sc. Tech.* 29 (2015), S. 1681–1688
- [23] Edelbrunner, H. ; Mücke, E.: Three-dimensional Alpha Shapes. In: *ACM Trans Graph* 12 (1994), S. 43–72